paring the SCF total energies obtained by using the 4-31G basis set for propane,[1,4] propene,[7] the *n*-propyl radical, and the hydrogen atom.[8] In this manner, the computed energies for eq 1 and 2 are 37 and 82 kcal/mol, respectively.

In contrast to the *n*-propyl radical is the energy required for C–H bond rupture in cubane and the cubyl radical, i.e., for reactions 3 and 4. Since experimental measurements

$$C_8H_8 \rightarrow C_8H_7\cdot + H\cdot \quad (3)$$

$$C_8H_7\cdot \rightarrow C_8H_6 + H\cdot \quad (4)$$

are not available for this system, the results of the ab initio calculations in this report will be used. When one uses the total energies for cubane, cubene, and the cubyl radical, the ΔH for rupture of a C–H bond in cubane, as indicated in eq 3, is found to be 91 kcal/mol. The ΔH for the β C–H bond scission reaction in the cubyl radical, as shown in eq 4, is 106 kcal/mol. Because of the neglect of correlation energy in the SCF total energies, only two significant statements may be made about the energetics of reactions 3 and 4. The first is that the C–H bond energies in cubane and the cubyl radical are about equal. The second is that the energy required for β C–H scission is clearly much higher than that for the other alkyl radicals discussed above.

The cubyl radical should therefore behave quite differently from alkyl radicals. Whereas a long C–H bond in a β position to the radical site is found for alkyl radicals, no such long C–H bond is found for the cubyl radical. If the long C–H bond in alkyl radicals indicates that the radical itself looks much like the transition state for the reaction toward the alkene, β C–H bond scission in the cubyl radical should not be an important thermal reaction. This view is supported by the binding energies for C–H bonds in a β position to the radical site. For the cubyl radical, it is found that the β C–H bonds remain strong, indicating that the cubyl radical should not readily form cubene by dissociating another hydrogen.

Conclusions

The only significant structural changes that occur when an open shell is formed in cubane is that the radical center has a more planar geometry with shorter α C–C bonds. Unlike the situation in other alkyl radicals, like, for example, the ethyl, *n*-propyl, and *tert*-butyl radicals, the β C–H bonds in the cubyl radical have the same length as those in cubane. Since the energy required for the β C–H bond scission is approximately that required for the dissociation of a C–H bond in cubane, then the geometry of the cubyl radical is probably not affected by the transition state for this reaction.

(7) Total energy for propene was taken from J. S. Binkley, J. A. Pople, and W. J. Hehre, *Chem. Phys. Lett.*, **36**, 1 (1975).
(8) R. Ditchfield, W. J. Hehre, and J. A. Pople, *J. Chem. Phys.*, **54**, 724 (1971).

Rate Constants, Branching Ratios, and Energy Disposal for Nf(b,a,X) and HF(*v*) Formation from the H + NF_2 Reaction

R. J. Malins[†] and D. W. Setser*

Department of Chemistry, Kansas State University, Manhattan, Kansas 66506 *(Received: December 2, 1980)*

The rate constant and energy disposal for the H + NF_2 reaction has been measured by observing infrared and visible chemiluminescence in a fast-flow, low concentration, flowing-afterglow apparatus at room temperature. The rate constant was determined by comparing the HF(v) emission intensity to the HCl(v) emission intensity from the H + Cl_2 reaction. The rate constant for formation of HF($v \geq 1$) is 3.8×10^{-12} cm^3 molecule^{-1} s^{-1}. Allowance for HF(v=0) formation gives a total rate constant which is about a factor of 3 larger. The observed HF(v_1,v_2,v_3,v_4) distribution is 0.75:0.20:0.04:0.01. The NF($a^1\Delta$–$X^3\Sigma^-$) emission also was observed; the NF($a^1\Delta$) vibrational distribution is v_0:v_1:v_2 = 0.73:0.19:0.08. Comparison of the NF($b^1\Sigma^+$) and NF($a^1\Delta$) emission intensities and using the HF(v=4) emission, which is energetically allowed only for formation of NF($X^3\Sigma^-$), gave NF(X):NF(a):NF(b) branching fractions of 0.07:0.91:0.02. By comparing the NF($a^1\Delta$–$X^3\Sigma^-$) intensity from H + NF_2 to the HF(3–0) emission intensity from the H + ClF reaction and by using the known rate constant and energy disposal for H + ClF, the radiative lifetime of NF($a^1\Delta$) was determined to be ~5.6 s. The 0–0, 1–1, and 2–2 band wavelengths of the NF($a^1\Delta$–$X^3\Sigma^-$) transition yielded $\omega_e' = 1184$ cm^{-1} and $\omega_e'x_e' = 8.5$ cm^{-1}.

Introduction

Reactions which generate electronically excited-state products have received considerable interest recently because of their potential application as chemical pumps for lasers. For less applied reasons, such reactions are of interest because the chemiluminscence identifies the populations in the product quantum states, which serves as an excellent probe of the reactions dynamics. Few chemical reactions give chemiluminescence that permits observation of all products; however, one example is hydrogen atoms plus NF_2 radicals which generates electronically excited NF and vibrationally excited HF products.[1-4] The internal energy of both HF and NF can be

[†] Air Force Weapons Laboratory, Kirtland Air Force Base, NM 87117.

(1) J. M. Herbelin and N. Cohen, *Chem. Phys. Lett.*, **20**, 605 (1973).
(2) J. M. Herbelin, *Chem. Phys. Lett.*, **42**, 367 (1976).
(3) M. A. Kwok and J. M. Herbelin in "Electronic Transition Lasers II", L. E. Wilson, S. N. Suchard, and J. I. Steinfeld, Ed., MIT Press, Boston, 1977.

0022-3654/81/2085-1342$01.25/0

assigned from the chemiluminescence and the translational energy obtained by subtraction from the available energy.

In this study we have measured the rate constant, k_{total}, for formation of HF($v \geq 1$) from the reaction of H with NF_2 by observing the HF infrared chemiluminescence and comparing this emission intensity to that from H + Cl_2.

$$H + NF_2 \xrightarrow{k_X} HF(v) + NF(X^3\Sigma^-) \quad (1a)$$

$$\Delta H^\circ_0 = -66 \text{ kcal mol}^{-1}$$

$$H + NF_2 \xrightarrow{k_a} HF(v) + NF(a^1\Delta) \quad (1b)$$

$$\Delta H^\circ_0 = -34 \text{ kcal mol}^{-1}$$

$$H + NF_2 \xrightarrow{k_b} HF(v) + NF(b^1\Sigma^+) \quad (1c)$$

$$\Delta H^\circ_0 = -13 \text{ kcal mol}^{-1}$$

$$k_{total} = k_X + k_a + k_b$$

In addition, the ratios of the individual rate constants, k_X, k_a, and k_b, were estimated. Since reaction 1b is dominant, the observed HF(v) distribution obtained from the HF(v) infrared chemiluminescence mainly applies to this channel. Vibrational distributions for HF(v), NF($a^1\Delta$), and NF($b^1\Sigma$) were determined. This study initially was begun as part of our continuing interest in the dynamics of halogen abstraction by H atoms.[5-7] Earlier work[1-3] had suggested that the reaction proceeded through an $HNF_2^\dagger$ intermediate complex, and that the energy disposal should be dominated by the dynamics of the unimolecular breakdown of $HNF_2^\dagger$. Presumably the favoring of the lowest NF singlet state, rather than the lowest triplet state, is a consequence of the bound $HNF_2^\dagger$ intermediate being a singlet state. The $HNF_2^\dagger$ triplet surface correlating to H + NF_2 is likely to be repulsive and not of importance.

Our flowing-afterglow, arrested vibrational relaxation apparatus,[5-7] which uses a Fourier transform spectrometer to observe the infrared emission, is well suited to studying reaction 1 because the observation time is sufficiently short to prevent vibrational and electronic relaxation of the long-lived NF(a,b) and HF(v) states. In this work a monochromator was added to observe the electronic transitions. The monochromator was placed on the opposite side of the flow reactor from the FT spectrometer. Thus, we were able to simultaneously observe the NF($a^1\Delta$–$X^3\Sigma^-$), NF($b^1\Sigma^+$–$X^3\Sigma^-$), and HF(v) transitions. Observation of NF($a^1\Delta$) in previous studies[1-3] was severely hindered by HF(Δv=3) overtone emission which occurs near the NF($a^1\Delta$–$X^3\Sigma^-$) bands. This problem was overcome by reducing the formation of HF(v) by controlling the H and NF_2 concentrations and by using a high flow velocity, which limits the secondary reactions. Observation of the NF($a^1\Delta$–$X^3\Sigma^-$) transition permitted the kinetics of NF(a) to be studied and also resulted in the determination of some spectroscopic parameters. In addition to values for ω_e' and $\omega_e'x_e'$, an estimate was obtained for the NF($a^1\Delta$) radiative lifetime. This was done by comparing the NF(a–X) emission intensity from a known concentration of NF_2 to the HF(Δv=3) emission intensity from H + ClF for the same H atom concentration.

Experimental Apparatus and Procedure

The experimental approach and data reduction were the same as that described in previous reports of the reactions of H atoms with X_2, XX′, and RX compounds.[5-7] The experiments were performed in a 55-mm o.d. Pyrex fast-flow reactor. Hydrogen atoms were admitted down the flow axis via a quartz tube and the NF_2, Cl_2, or ClF was admitted via a Pyrex ring concentric with the reactor axis and having holes on its inner surface. Emission was observed transverse to flow through NaCl windows; the observation area was 1 cm downstream of the reagent inlet ring. A diagram and discussion of specific details is given in ref 5. A Roots-type blower was used to maintain flow velocities of ~90 m s^{-1}. This flow velocity corresponds to a reaction time of ~0.24 ms between the mixing ring and observation point. The N_2F_4, Cl_2, or ClF were premixed with Ar and stored in reservoirs. The Ar carrier gas was added to the flow reactor via the hydrogen flow train and also via an additional Pyrex ring upstream of the mixing zone. Total Ar flow was ~7 mmol s^{-1}; the total reactor pressure was 0.7 torr. Reagent flows were in the range 0.1–5 μmol s^{-1}, which corresponds to a concentration range of 0.3×10^{12}–15×10^{12} molecules cm^{-3}. Hydrogen was dissociated by a microwave discharge 18 cm upstream of the mixing zone. Assuming 50% dissociation, [H] was ~2×10^{12} atoms cm^{-3}.

The NF_2 was generated by thermal dissociation of N_2F_4 in a thoroughly passivated stainless-steel gas-handling line. The N_2F_4 was obtained from AerospaceCorp. as a gift. The N_2F_4 was of 97% purity with the major impurities being N_2 and F_2. These were removed by freezing the sample at liquid N_2 temperature and pumping for several minutes. The sample was then cryongenically transferred into a stainless-steel vacuum system, with the cold trap maintained well below room temperature. After transferring to the stainless steel reservoir, the sample was again pumped while at liquid N_2 temperature. After warming to room temperature, the N_2F_4 was diluted with dry Ar. During an experiment, the entire stainless-steel vacuum system including lead lines up to and *inside the flow reactor* were heated to 230 °C in order to totally dissociate the N_2F_4 to NF_2. The NF_2/Ar reservoir was heated with a resistance furnace; the remainder of the stainless vacuum system was heated with commerical heating tapes and the lead lines were heated with nichrome wire. The temperature was measured on the outer wall of the stainless reservoir after 3 h heating time had been allowed for equilibration with the reservoir's contents. This arrangement was satisfactory for handling of N_2F_4/NF_2. However, even dilute samples of N_2F_4 may react explosively with hydrocarbons and care always must be exercised in handling N_2F_4.

The chlorine was obtained from Matheson and was used without purification. The ClF was taken from a tank obtained from Ozark Mahoney Co. This ClF tank was previously used for the study of metastable rare gas atom reactions with ClF. In these reactions characteristic emissions identify the presence of Cl_2. According to this test, the ClF tank had no detectable Cl_2 impurity which means that Cl_2 was below the 1% level. Any F_2 impurity would be of no consequence for the lifetime measurements because the H + F_2 rate constant is 300 times less than that of H + ClF. The argon carrier gas was purified by passage through molecular sieve traps at low pressure.

Relative rate constants for HF(v) and HCl(v) formation at 300 K were determined by monitoring the emission

(4) M. A. A. Clyne and I. F. White, *Chem. Phys. Lett.*, **6**, 465 (1970); (b) C. T. Cheah, M. A. A. Clyne, and P. D. Whitefield, *J. Chem. Soc., Faraday Trans. 2*, **76**, 711 (1980); (c) C. T. Cheah and M. A. A. Clyne, *ibid.*, in press.

(5) J. P. Sung, R. J. Malins, and D. W. Setser, *J. Phys. Chem.*, **83**, 1007 (1979).

(6) (a) J. P. Sung and D. W. Setser, *Chem. Phys. Lett.*, **58**, 98 (1978); (b) J. P. Sung, D. W. Setser, and H. Heydtmann, *Ber. Bunsenges. Phys. Chem.*, **83**, 1272 (1979).

(7) R. J. Malins and D. W. Setser, *J. Chem. Phys.*, in press.

intensity as a function of reagent flow with the Digilab FTS-20 Fourier transform spectrometer under conditions of constant H atom concentration. The response of the system was calibrated with a black-body standard. Individual rotational lines were converted to vibrational populations and then to total emission intensity in the following manner. Because of the high resoltuion of the FTS and the Boltzmann rotational distributions, the relative vibrational populations were determined by choosing several appropriate rotational lines (appropriate in the sense that they were not obscured by CO_2 or H_2O absorption) of each v level and measuring their heights. Dividing by the product of the Einstein coefficient[8] for spontaneous emission, the detector response function, and the Boltzmann fraction for that J state converts the peak height to a relative population for that v level. The rotational lines belonging to the same v level were averaged to give a final result. The relative vibrational populations were then summed to give a total relative $HX(v\geq1)$ concentration. Relative rate constants were obtained by comparing the slope from the plot of total relative HX concentration vs. RX flow for NF_2 with the slope obtained from a plot of the H + Cl_2 reaction under the same experimental conditions.

The visible emission was observed simultaneously with the IR emission by a 0.3-m McPherson monochromator with a grating blazed at 10 000 Å. The detector was an RCA C31034 photomultiplier tube, which has good sensitivity in the 8000–9000-Å range, operated in the photon-counting mode. The assembly of mirrors and monochromator was mounted on a wheeled table, which could be rolled from one reactor window to the next, allowing emission to be monitored as a function of distance along the tublar reactor. The monochromator was used for observing the $NF(b^1\Sigma^+)$ emission at 520–530 nm, the $NF(a^1\Delta)$ emission at 880–870 nm, and HF(3–0) emission at 890–870 nm.

The radiative lifetime measurements consisted of comparing the $NF(a^1\Delta-X^3\Sigma^-)$ emission from H + NF_2 with the HF(3–0) emission from the H + ClF reaction under identical reaction conditions at the first window of the flow tube. While the visible emission spectra were being obtained, $HF(\Delta v=1)$ infrared spectra were taken simultaneously from the opposite side of the window. The simultaneous collection of the infrared and visible spectra allows the unequivocal determination of the relative population of $HF(v=3)$ from the ClF reaction, as well as verifying that the conditions for the H + NF_2 experiment were satisfactory. The method of calculating the radiative lifetime of $NF(a^1\Delta)$ from these spectra is discussed in the next section.

Results

Infrared Emission and Total Rate Constant. The different NF_2 mixtures were used to determine a total of four values for the room temperature rate constant for the H + NF_2 reaction. The four results agreed to within 10% and yielded a rate constant for $HF(v\geq1)$ formation of 3.8 $\times 10^{-12}$ cm^3 $molecule^{-1}$ s^{-1} (based on a rate constant of 2.06 $\times 10^{11}$ cm^3 $molecule^{-1}$ s^{-1} for H + Cl_2).[8,9] Some of the data from which the rate constants were derived are presented in Figure 1; the $HF(v)$ and $HCl(v)$ concentrations are linear in NF_2 ($NF_2 = 2N_2F_4$) and Cl_2 flows, respectively. Since the [H] are the same, the ratio of the slopes of these plots gives the ratio of rate constants for formation of $HF(v\geq0)$

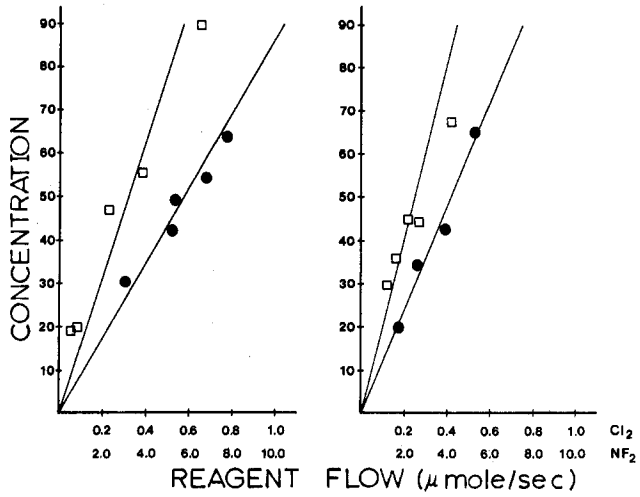

Figure 1. Comparison of HCl and HF emission intensities from the H + Cl_2 (●) and H + NF_2 (□) reactions for two experiments; a flow of 1.0 μmol s^{-1} is equivalent to a concentration of 3.2 $\times 10^{12}$ molecule cm^{-3}.

and $HCl(v\geq0)$. There are three possible sources of error to the $HF(v\geq1)$ formation rate constant: reduction of the emission spectra to relative concentrations, preparation of the N_2F_4 sample, and incomplete dissociation of N_2F_4 to NF_2. We have employed relative HF and HCl chemiluminescence emission measurement to determine rate constants for several reactions.[5] The HCl and HF Einstein coefficients and the data reduction procedure are reliable, as judged by comparing the relative rate constants to other measurements in the literature. Estimation of possible errors resulting from gas handling is difficult; however, since different mixtures gave the same result the techniques seem to be satisfactory. The major uncertainty probably is the assumption of 100% dissociation of N_2F_4 to NF_2. Recent thermodynamic[11,12] and kinetic studies[13] have shown that, above 500 K, N_2F_4 is essentially 100% dissociated. We took every precaution to ensure dissociation by heating the entire N_2F_4 reservoir, all lead lines to the flow reactor, and the short line inside the reactor wall extending from the reactor wall to the Pyrex nozzle. Furthermore, we allowed 3–4-h warm-up periods to ensure that the entire gas sample was homogeneously heated. We estimate that there should be less than 15% uncertainty in the rate constant from incomplete dissociation. If we take account of all these possibilities, the uncertainty in the $HF(v\geq1)$ formation rate constant ratio is estimated as ±30%. The major difficulty in obtaining the total rate constant is in estimating the relative amount of $HF(v=0)$ that is produced by reaction 1. The $HCl(v=0)$ from H + Cl_2 is insignificant. The $HF(v)$ and $DF(v)$ distributions from H and D atoms with NF_2 are listed in Table I and plotted in Figure 2. We observed no variation of the $HF(v)$ distribution with $[NF_2]$, as shown in Figure 3. The constant population ratios actually extend to quite high NF_2 concentration relative to many polyatomic reagents, which frequently start to give relaxation at $\gtrsim 5 \times 10^{12}$ molecules cm^{-3}. The $HF(v)$ and $DF(v)$ distributions vary almost exponentially with energy, and a log P_v vs. E_v can

(8) K. Tamagake and D. W. Setser, *J. Phys. Chem.*, **81**, 100 (1979).
(9) P. P. Bemand and M. A. A. Clyne, *J. Chem. Soc., Faraday Trans. 2*, **73**, 394 (1977).
(10) H. G. Wagner, U. Welzbacher, and R. Zellner, *Ber. bunsenges. Phys. Chem.*, **80**, 902 (1976).
(11) D. J. Evans and E. Tschuikow-Roux, *J. Phys. Chem.*, **82**, 182 (1978).
(12) J. H. Piette, F. A. Johnson, K. A. Booman, and C. B. Colburn, *J. Chem. Phys.*, **35**, 1481 (1961).
(13) E. Tschuikow-Roux, K. O. McFadden, K. H. Jung, and D. A. Armstrong, *J. Phys. Chem.*, **77**, 734 (1973).

TABLE I: HF and DF Vibrational Distributions

reaction	$\langle E \rangle$,[a] kcal/mol	$\langle f_V \rangle$	$\langle f_R \rangle$[b]	P_V v_0	v_1 v_1	v_2	v_3	v_4
H + NF_2	36				0.75[c]	0.20[c]	0.04[c]	0.01[c]
	36	0.12	~0.03	0.71[d]	0.22	0.06	0.01	0.003
	36	0.14	~0.03	0.65[e]	0.27	0.07	0.01	
D + NF_2	37				0.58[c]	0.27	0.13	0.02
	37	0.15	~0.03	0.56[d]	0.25	0.12	0.06	0.01
		0.17	~0.03	0.51[e]	0.28	0.14	0.06	0.01

[a] Assuming a 1 kcal mol^{-1} activation energy and $\langle E \rangle = \Delta H^\circ_0 + E_a + {}^5/_2RT$. [b] Calculated as upper limit assuming $J \leq 10$ a and that the rotational distribution is roughly symmetric and peaked at $J = 5$. [c] Observed distribution. [d] Obtained by extrapolation of graph of ln (P_V) vs. E_V, see Figure 2; $P_V = 4$ is ignored in calculating $\langle f_V \rangle$. [e] Obtained by extrapolation of surprisal plot, see Figure 2 and text. Within the experimental uncertainty, subtraction of the HF(v) component associated with NF(X) formation has no effect on $\langle f_V \rangle$.

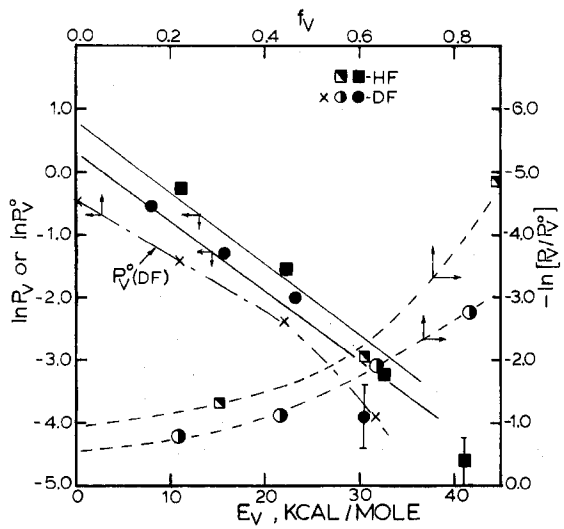

Figure 2. Plots of the experimental HF(v) and DF(v) populations, P_V, vs. E_V. The prior (four-body case) distribution, for DF, and surprisal plots vs. f_V also are shown. The $v = 0$ population is not included in the normalization of the experimental distribution, but it is included in the DF prior. The $v = 4$ point for the prior is off scale and not shown.

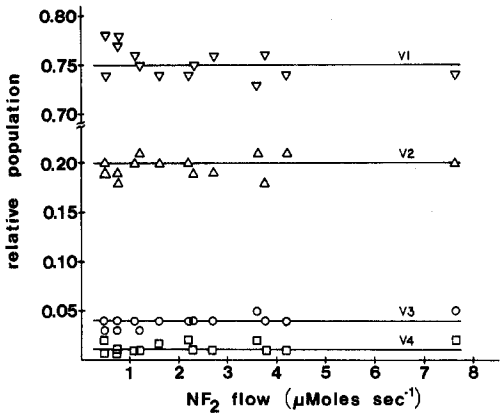

Figure 3. Variation of P_V(HF) with NF_2 flow rate (or concentration, 1 μmol s^{-1} is equivalent to 3.2×10^{12} molecule cm^{-3}).

be used to estimate the relative $v = 0$ population; these give 71 and 56% for HF(v=0) and DF(v=0), respectively. Another common way to estimate the $v = 0$ contribution is to extrapolate surprisal plots. The surprisal plots (for the four-body HF + NF(a) prior) also are shown in Figure 2 for the HF and DF distributions. Although the plots are not linear, smooth extrapolations to $f_V = 0$ still can be made. For these extrapolations 65 and 52% of the HF and DF, respectively, are formed in $v = 0$. Thus, the observed rate constant for HF($v \geq 1$) formation should be increased by a factor of ~3 and $k_{total} = 1.3 \times 10^{-11}$ cm^3 $molecule^{-1}$ s^{-1} with an uncertainty of ±50%.

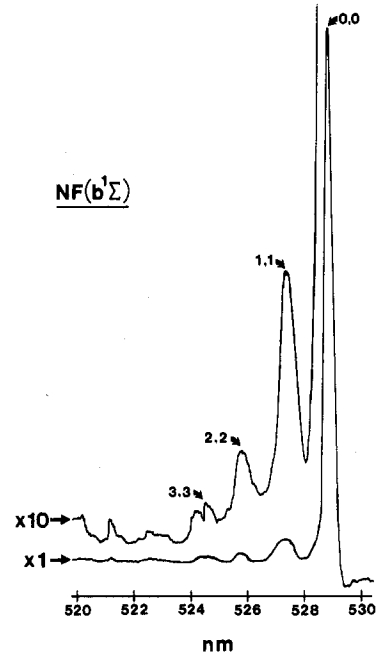

Figure 4. The NF($b^1\Sigma^+$–$X^3\Sigma^-$) emission spectrum from H + NF_2 observed at first window. The flow rate for NF_2 was 1.4 μmol s^{-1} or [NF_2] = 4.5×10^{12} molecules cm^{-3}.

There was no observable emission from HF($v \geq 5$). For our signal-to-noise ratio and the HF(v=5) radiative lifetime, an upper bound to the relative HF($v \geq 5$) population is 0.001. This limit is important because formation of NF($X^3\Sigma^-$) permits excitation up to HF(v=6); whereas, reaction 1b gives only $v \leq 3$. The observation of HF(v=4) is interpreted to mean that a small fraction of the reaction proceeds via reaction 1a. Emission from DF(v) levels sufficiently high to prove NF($X^3\Sigma^-$) formation was not observed; however, only a few D + NF_2 experiments were done and this failure to see DF($v \geq 5$) is not viewed as a contradiction to the claim of NF($X^3\Sigma^-$) formation from the observation of HF(v=4). The k_{1a}/k_{1b} ratio will be estimated in the Discussion section.

NF($a^1\Delta$–$X^3\Sigma^-$) and NF($b^1\Sigma^+$–$X^3\Sigma^-$) Emissions. The visible emission from the H + NF_2 reaction is quite striking to the eye. Even for fast-flow conditions, the entire flow reactor from the reagent nozzle to the pump inlet appeared deep green in a darkened room. As the H atom concentration was increased from 2×10^{12} to 20×10^{12} atoms cm^{-3}, the green NF($b^1\Sigma$–$X^3\Sigma^-$) emission was slowly replaced by a yellow glow, which arises from the N_2($B^3\Pi_g$–$A^3\Sigma_u^+$) emission. Some typical spectra obtained at the first window for low [H] and [NF_2] are shown in Figures 4 and 5. The NF($b^1\Sigma^+$–$X^3\Sigma^-$) spectrum is the same

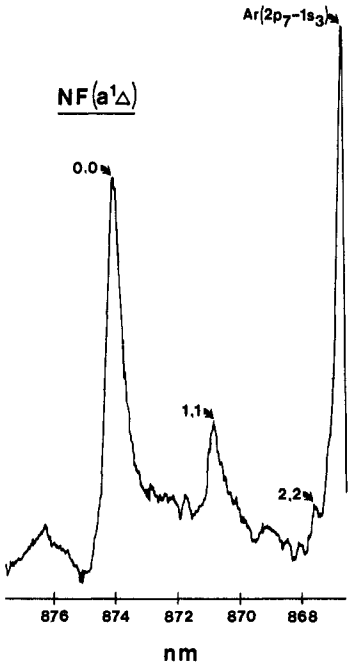

Figure 5. NF($a^1\Delta$–$X^3\Sigma^-$) emission spectrum from H + NF_2 observed at first window. The peak positions of the bands are 0–0 = 874.2 nm, 1–1 = 870.9 nm, and 2–2 = 867.6 nm. The wavelength scale of the monochromator was calibrated by the 0–0 band of the a–X transition and the positions of the Ar and HF(Δv=3) lines. The flow rate for NF_2 was 1.4 μmol s^{-1} for a [NF_2] of 4.5 × 10^{12} molecules cm^{-3}.

TABLE II: Vibrational Distributions[a] for NF($a^1\Delta$) and NF($b^1\Sigma^+$)

product	⟨E⟩	⟨f_V⟩	v_0	v_1	v_2	v_3
NF($a^1\Delta$)[b]	36		0.73	0.19	0.08	d
NF($b^1\Sigma^+$)[c]	15		0.95	0.04	0.01	0.003

[a] Since the equilibrium internuclear distance for NF(X), NF(a), and NF(b) states are similar, the Franck–Condon factors for Δv = 0 transitions should be roughly constant. Hence the ratios of emission intensities for the different vibrational levels were equated with the relative vibrational populations. [b] Calculated from the ratios of peak areas measured with a planimeter. [c] Calculated from the ratios of peak heights. [d] Other emissions would have prevented the observation of the 3–3 band.

as previously reported;[14] the 0–0 band is the strongest and is followed by exponentially declining intensities for the 1–1, 2–2, and 3–3 bands. The NF($a^1\Delta$–$X^3\Sigma^-$) spectrum has not been reported in earlier work because it was overlapped by strong HF(3–0) emission[1-4] from the F + H_2 reaction, which was used to generate H atoms. Only the 0–0 band has been reported in the literature; but the 0–0, 1–1, and 2–2 bands are apparent in Figure 4. From these wavelengths and the known[15,16] spectroscopic constants of NF(X), ω_e' and $\omega_e'x_e'$ for NF($a^1\Delta$) were calculated as 1184 and 8.5 cm^{-1}, respectively. The intensities of the NF($b^1\Sigma^+$) and NF($a^1\Delta$) bands decline exponentially. Since the potential curves of the X, a, and b states have essentially the same equilibrium bond length,[14-17] the Franck–Condon factors for the 0–0, 1–1, and 2–2 transitions of b–X and a–X systems should be nearly equal and the ratio of the

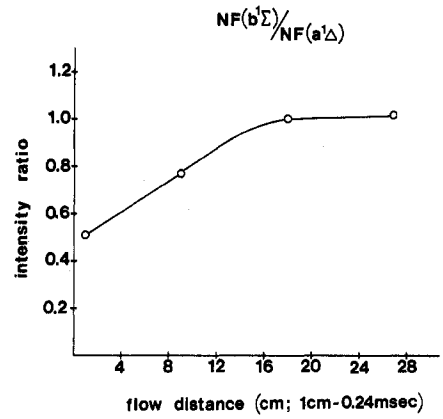

Figure 6. NF(b–X)/NF(a–X) intensity ratio vs. distance in the flow reactor. This ratio has not been corrected for wavelength response of the detection system. The NF_2 flow was 3.2 μmol s^{-1} for [NF_2] = 1.0 × 10^{13} molecules cm^{-3}.

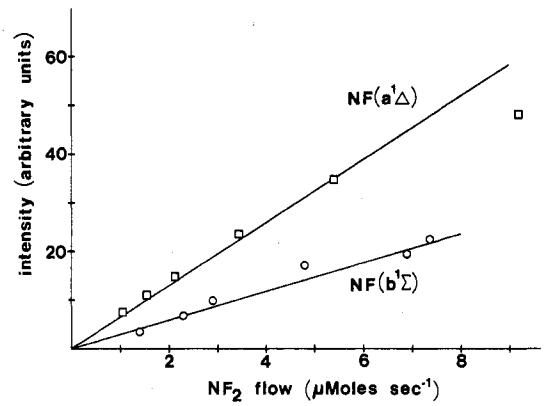

Figure 7. Variation of the NF(b–X) and NF(a–X) emission intensities at the first window with NF_2 concentration.

peak heights should be essentially the ratio of the vibrational populations. The peak height ratios are given in Table II as relative vibrational populations.

The 0–0 band emission intensity from both excited NF states was monitored vs. NF_2 concentration at the first window (reaction time ~ 0.2 ms) under two conditions: (1) high bulk flow velocity and moderate NF_2 flows, 1 × 10^{12}–6 × 10^{12} molecules cm^{-3} and (2) slow bulk velocity and very low NF_2 flows. The monochromator slits were set at 80 μm to prevent interference from other bands. The former set of data is plotted in Figure 6. Under both conditions the emission intensity of NF($a^1\Delta$) and NF($b^1\Sigma^+$) was linear in [NF_2], providing that [NF_2] was ≤10^{13} molecule cm^{-3}.

The NF(b–X) and NF(a–X) emission intensity ratio was measured as a function of flow distance in the reactor by moving the monochromator to various windows. A representative experiment is displayed in Figure 7; the ratio has not been corrected for the variation of the detector response with wavelength. The NF(b)/NF(a) ratio increases with distance. This experiment was repeated several times and a smooth increase was observed on each occasion.

Radiative Lifetime Determination of NF($a^1\Delta$). The radiative lifetime of NF($a^1\Delta$) was measured by comparing the NF(a–X) emission intensity from a known concentration of NF(a) with the Δv=3 emission intensity from a known concentration of HF(v=3). The H + ClF reaction was selected for the HF source because (i) the rate constant has been measured, (ii) the gas handling is relatively straightforward, and (iii) the branching fraction and vibrational distributions are known.[5,18]

(14) A. E. Douglas and W. E. Jones, *Can. J. Phys.*, **44**, 2251 (1966).
(15) B. Rosen, Ed., "International Table of Selected Constants. 17. Spectroscopic Data Relative to Diatomic Molecules", Pergamon Press, New York, 1970.
(16) S. N. Suchard, "Spectroscopic Constants for Selected Heteronuclear Diatomic Molecules", Aerospace Report No. TR-0074(4641)-6, Aerospace Corp., El Segunda, CA.
(17) W. E. Jones, *Can. J. Phys.*, **45**, 21 (1967).

$$H + ClF \rightarrow HCl(v) + F \quad (2)$$

$$v_1/v_2/v_3/v_4 = 0.16/0.33/0.39/0.12$$

$$k_{HCl} = 3.4 \times 10^{-11}\ cm^3\ molecule^{-1}\ s^{-1}$$

$$H + ClF \rightarrow HF(v) + Cl$$

$$v_1/v_2/v_3/v_4/v_5/v_6 = 0.04/0.08/0.12/0.25/0.39/0.19$$

$$k_{HF} = 0.66 \times 10^{-11}\ cm^3\ molecule^{-1}\ s^{-1}$$

Because of interfering background emission, only the P_1 to P_3 lines of the 3–0 HF band could be compared to the NF(a–X) emission. The ratio of the HF(3,3–0,2) and NF(a–X) emission intensities were selected for quantitative study; this ratio is the product of the Einstein coefficient ratio and the molecular concentration ratio.

$$I^{NF}/I^{HF} = A(NF,a)[NF(a^1\Delta)]\{A_0^3{}_{J'}^{J'}[HF(v'=3,J'=3)]\}^{-1} \quad (3)$$

Since the intensity ratio was measured under conditions of short observation time and equal [H], the HF(v=3) and NF(a) concentrations may be expressed in terms of the product formation rate constants, the reagent concentrations, the reaction time, and branching fraction for the HF(v'=3,J'=3) concentration.

$$[NF(a^1\Delta)] = k_a[H][NF]\Delta t \quad (4)$$

$$[HF(3,3)] = k_{HF}[H][ClF]\Delta t P_{v=3} F_B(J'=3) \quad (5)$$

$P_{v=3}$ is the relative population of HF(v=3), and $F_B(J'=3)$ is the Boltzmann fraction for $J' = 3$ of $v' = 3$. Substituting eq 4 and 5 into eq 3 and solving for the Einstein coefficient for NF($a^1\Delta$), gives eq 6. The HF(3,3–0,2) line at 879.2 nm

$$A(NF,a) = A_0^3{}_{J'}^{J'}(HF)(I^{NF}/I^{HF}) \times (k_{HF}/k_a)([CLF]/[NF_2])(P_{v=3}F_B(J'=3)) \quad (6)$$

was used and the value for $P_{v=3}$ was directly determined from the HF(Δv=1) emission that was observed with the interferometer simultaneously with the visible emission measurements. The branching fraction for $a^1\Delta$ was taken as unity and our estimate for $k_a = 1.3 \times 10^{-11}$ cm^3 molecule^{-1} s^{-1} was used. the value[19] for $A_0^3{}_{J''=2}^{J'=3}$ is 0.53 s^{-1}. The observed HF(v) distribution was 0.08/0.13/0.18/0.24/0.24/0.23/0.14 for $v_1/v_2/v_3/v_4/v_5/v_6$ at [ClF] = 9.0×10^{12} molecules cm^{-3}. This distribution is somewhat relaxed from the HF(v) distribution listed under eq 2. The relaxation results from the high ClF concentration, which was necessary to obtain strong $\Delta v = 3$ emission intensity. In order to verify that relaxation of HF(v) did not affect the present results, the HF($v \geq 1$) formation rate constant from H + ClF, relative to that for H + Cl_2, was measured for the high ClF flows used for the NF_2 experiments. This measurement yielded a rate constant for H + ClF which was slightly lower than our published value, but still within the experimental error. Furthermore, the total HX(v) intensity was linear in [ClF] and the HF formation branching ratio was only slightly higher than our previously published value. Thus, we conclude that the present data from the H + ClF reaction are satisfactory, and that the minor relaxation of the HF(v) distribution will contribute little experimental error, since the formation of HF(v=3) that was actually present, as determined simultaneously with the visible emission measurement, was used in eq 6.

Consequently experiments were done with H + ClF and H + NF_2 for identical experimental conditions; i.e., same monochromator position and same slit width and the same [H]. The peak areas were used as intensities in eq 6; the areas were obtained by planimeter reeadings. Four separate experiments were done yielding 5.6 ± 0.6 s for the radiative lifetime of NF($a^1\Delta$). Additional values were obtained from the peak height vs. [NF_2] data by running a ClF spectrum at the same conditions, estimating the NF($a^1\Delta$) peak area from the peak height and the average ratio of peak areas to peak height, and measuring the HF(3,3–0,2) emission intensities. These calculations yielded a value of ~5.8 s for the NF($a^1\Delta$) lifetime. Based only on the scatter of data points, the uncertainty is ±10%; however, the systematic error certainly is much larger. The measured lifetime depends upon the values for both rate constants, A_0^3(HF) and the NF_2 and ClF concentrations. The estimate of the HF(v=0) contribution to the total NF(a) formation rate constant probably is the source of the greatest uncertainty.

Discussion

Clyne and co-workers[4b] have reported a H + NF_2 rate constant, based on measurement of H atom removal, of (1.5 ± 0.2) × 10^{-11} cm^3 molecule^{-1} s^{-1} that closely agrees with our rate constant (including formation of HF(v=0)) of 1.3 × 10^{-11} cm^3 molecule^{-1} s^{-1}. Conversely, we could argue that the close agreement supports our estimate for the contribution from HF(v=0) formation. At first glance a value of 1 × 10^{-11}–2 × 10^{-11} is surprisingly low because the H + NF_2 reaction may be viewed as a radical combination reaction, which normally have rate constants near the gas kinetic collision number. In fact, considering H + NF_2 as a radical combination process is supported by its very low (~0 kcal mol^{-1}) activation energy.[4b] Other[20] H atom reactions with small stable inorganic radicals (H + NO_2, k = 13 × 10^{-11} cm^3 molecule^{-1} s^{-1} and H + ClO_2, k = 5.9 × 10^{-11} cm^3 molecule^{-1} s^{-1}) are somewhat faster than H + NF_2. However, the rate constant[21] for OH + NO_2 is 1.6 × 10^{-11} cm^3 molecule^{-1} s^{-1}. Thus, relative to other small inorganic radicals the H + NF_2 rate constant is low, but not anomalously low. Before continuing, the intermediate complex mechanism should be examined. In order for $k_2 = k_1$, $k_2 > k_3[M]$ and k_{-1}. In fact if $k_{-1} \approx k_2$ (reaction 7)

$$\begin{array}{l} H + NF_2 \underset{k_{-1}}{\overset{k_1}{\rightleftharpoons}} HNF_2{}^\dagger \xrightarrow{k_2} HF + NF(a^1\Delta) \\ \qquad\qquad\qquad\quad \downarrow k_3[M] \\ \qquad\qquad\qquad\quad HNF_2 \end{array} \quad (7)$$

then both the observed rate of [H] removal and rate of HF formation would be less than the true bimolecular rate associated with k_1.

In order to make an RRKM estimate of k_{-1} with k_2 the thermochemistry must be evaulated. Using $\Delta H_f{}^\circ{}_{298}(NF_2)$[22] = 10.7 and $\Delta H_f{}^\circ{}_{298}(HNF_2)$[23] = −15.6 kcal mol^{-1} gives ΔH_{298} = −78 kcal mol^{-1} for formation of $HNF_2{}^\dagger$ from H + NF_2. Thus, $HNF_2{}^\dagger$ has a vibrational energy of ≈78 kcal mol^{-1}. The threshold energies for the HF elimination steps are unknown; however, from the enthalpy of reaction 1b; E_0(NF(a)) must be ≥44 kcal mol^{-1}. The RRKM calcula-

(18) D. Brandt and J. C. Polanyi, *Chem. Phys.*, **35**, 23 (1978).

(19) Based on the values calculated by means of the numerical eigenfunction technique[8] and the rotationless Einstein emission coefficient for $A_0^3(m=0)$ of J. M. Herbelin and G. Emanuel, *J. Chem. Phys.*, **60**, 689 (1974).

(20) (a) M. A. A. Clyne and P. B. Monkhouse, *J. Chem. Soc., Faraday Trans. 2*, **73**, 298 (1977); (b) P. P. Bemand, M. A. A. Clyne, and R. T. Watson, *J. Chem. Soc., Faraday Trans. 1*, **69**, 1356 (1973).

(21) C. Anastasi and I. W. M. Smith, *J. Chem. Soc., Faraday Trans, 2*, **72**, 1459 (1976).

(22) D. R. Stull, Ed., "JANAF Thermochemical Tables", Dow Chemical Co., Midland MI, 1965 and supplements.

(23) A. V. Paukratov, A. N. Zercheneov, V. I. Chesnokov, and N. N. Zhdanova, *Russ. J. Phys. Chem.*, **43**, 212 (1969).

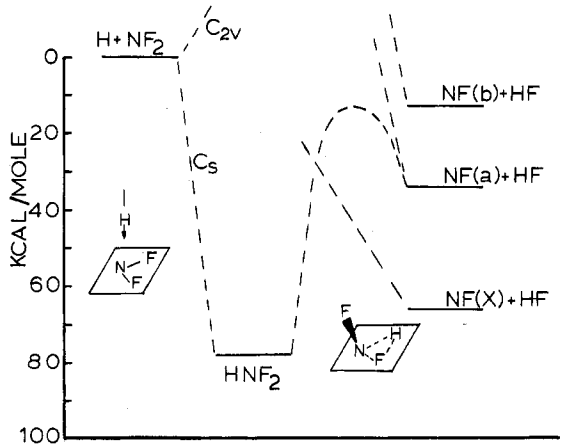

Figure 8. Reaction profile for the H + NF_2 reaction with emphasis on the anticipated high barrier for the reverse reaction of NF(a$^1\Delta$) with HF.

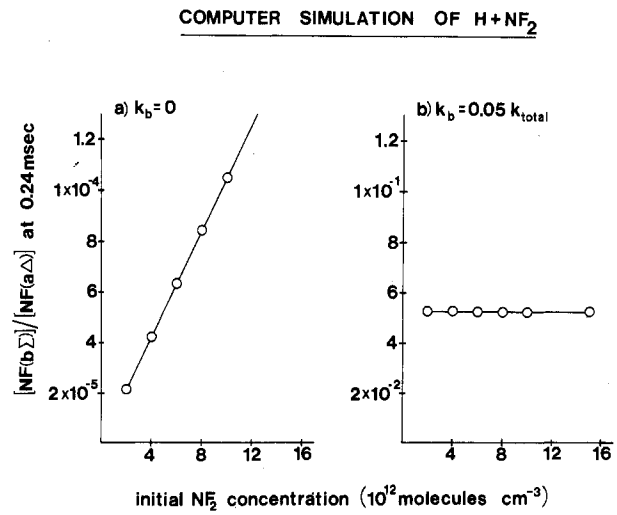

Figure 9. Computer simulation of the NF(b–X)/(NF(a–X) intensity ratio for two mechanisms of NF(b) formation: (a) excitation transfer from HF(v) and (b) direct formation. For mechanism a the transfer rate constant was set at the gas kinetic value.

tions[24] for k_{-1} were performed for a threshold energy of 55, 65, and 75 kcal mol^{-1}. The frequencies selected for HNF_2 and for the two activated complexes were based on the values give in ref 22 and 23 for NF_2 and HNF_2, respectively, to obtain preexponential factors (partition function form at 500 K) of 2.4×10^{13} and 2.1×10^{14} s^{-1} for elimination and redissociation, respectively. The HF elimination rate constants for an internal energy of 80 kcal mol^{-1} are 4.7×10^{11}, 6.6×10^{10}, and 2.4×10^{9} s^{-1} for E_0 = 55, 65, and 75 kcal mol^{-1}, respectively. The RRKM dissociation rate constant was 2.7×10^{9} s^{-1}. These rough calculations show that redissociation will not complete with elimination unless the threshold energy for HF elimination is within a few kcal mol^{-1} of the threshold energy for redissociation. Since other three-centered elimination reactions,[25-27] such as HX elimination from the halomethanes, have threshold energies only 5–10 kcal mol^{-1} in excess of the reaction endoergicity, it is unlikely that the threshold energy for the $HNF_2^{\dagger}$ is more than 20 kcal mol^{-1} in excess of the endoergicity, i.e., the barrier for the addition of NF(a$^1\Delta$) to HF is probably not larger than 20 kcal mol^{-1}. Thus, we conclude that redissociation of $HNF_2^{\dagger}$ is not of significance. At 1 torr of Ar the collision frequency is 3×10^{6} s^{-1}; so, collisional deactivation also is not competitive with HF elimination. We can thus equate our HF($v \geq 0$) formation rate constant with k_1.

The rather small rate constant, relative to the limiting gas kinetic value, must be associated with a steric factor since the activation energy is small.[4b] The bond angle in NF_2 is 105° but the unpaired electron still is in an orbital perpendicualr to the molecular plane. The approach of H in the NF_2 molecular plane toward the lone pair orbital in C_{2v} geometry is repulsive and correlates to an HNF_2 electronically excited state.[25] However, approach of H perpendicularly to the NF_2 plane in C_s geometry should lead to the HNF_2 ground electronic state. Thus, the small rate constant can be associated, at least in part, with an appreciable steric factor. Some aspects of the potential profile are summarized in Figure 8.

Branching Fractions for NF(X,a,b) Formation. Early studies[1-3] concluded that the majority of the NF product is formed in the a$^1\Delta$ state. Cheah and Clyne[4c] concluded that NF(a) was formed with a branching fraction > 0.9. Our data also are consistent with this conclusion. However, small amounts of both b and X states are formed directly. The direct formation of NF(X$^3\Sigma^-$) can be inferred from the presence of HF(v=4) emission. The ratio of HF(v=4) to HF(v<4) can be used to determine a lower limit to the NF(X)/NF(a) branching ratio. In a similar fashion, the I(NF,b–X)/I(NF,a–X) ratio allows the calculation of the NF(b)/NF(a) branching ratio, after allowance is made for the radiative lifetimes.

The presence of NF(b$^1\Sigma^+$) was attributed by Herbelin[1] to a near-resonant V–E transfer between HF($v \geq 2$) and NF(a$^1\Delta$). However, direct formation of NF(b$^1\Sigma^+$) can be inferred from our observed independence of NF(b$^1\Sigma^+$)/NF(a$^1\Delta$) on [NF_2]. We performed a computer simulation of NF(b) and NF(a) formation from the H + NF_2 system (see Figure 9) assuming either direct formation or collisional formation. If NF(b$^1\Sigma^+$) were formed only by collisional energy transfer, the NF(b)/NF(a) ratio would show a strong dependence on [NF_2]. On the other hand, if NF(b) is formed by direct reaction this ratio will be independent of [NF_2]. The latter matches our experimental results. Moreover, the calculations (Figure 9) show that even if the energy transfer rate constants are gas kinetic, the amount of NF(b$^1\Sigma^+$) formed by V–E transfer is insignificant because the concentration of HF($v \geq 2$) is very small. Using the observed intensity ratio of 0.51, our radiative lifetime for NF(a$^1\Delta$) and Clyne's radiative lifetime[4a] for NF(b$^1\Sigma^+$) of 0.2 s gives b$^1\Sigma^+$:a$^1\Delta$ = 1:32.

The assignment of the branching ratio for NF(X) is more difficult. The possible sources of HF(v=4) is formation by reaction 1a, HF(v) energy pooling, or secondary reactions. The concentrations of HF(v) molecules is far too small and the reaction time far too short for energy pooling to generate HF(v=4). We also can rule out the secondary reaction

$$H + NF(a^1\Delta) \rightarrow HF + N(^4S) \qquad (8)$$

$$\Delta H^\circ = -95 \text{ kcal mol}^{-1}$$

because Clyne and Cheah[4c] have shown that N(^{2}D) with ΔH° = −40 kcal mol^{-1}, is the product and that the rate constant is $(2.5 \pm 0.5) \times 10^{-13}$ cm^3 molecule^{-1} s^{-1}. The rate constant for this secondary reaction would have to be $\gtrsim 10^{-9}$ cm^3 molecule^{-1} s^{-1} for it to be the source of HF(v=4).

(24) P. J. Robinson and R. A. Holbrook, "Unimolecular Reactions", Wiley, New York, 1972.
(25) H. Okabe, "Photochemistry of Small Molecules", Wiley-Interscience, New York, 1978, p 79.
(26) B. E. Holmes and D. W. Setser in "Physical Chemistry of Fast Reactions", Vol. 2, I. W. M. Smith, Ed., Plenum, New York, 1980.
(27) (a) A. S. sudbo, P. A. Schulz, Y. R. Shen, and Y. T. Lee, *J. Chem. Phys.*, **69**, 2312 (1978); (b) C. R. Quick, Jr., and C. Wittig, *ibid.*, **72**, 1694 (1980).

Hence, the HF(v=4) must come from reaction 1a. The NF($X^3\Sigma^-$) is most likely formed via the same HNF_2* intermediate as the NF($a^1\Delta$) state but via a singlet–triplet surface crossing. Hence, the energy disposal to HF(v) from reaction 1a may be similar to that from reaction 1b. If one assumes that the HF(v) distribution from reaction 1a is an exponential declining function of f_V and has the same $\langle f_V \rangle$ as reaction 1b, one can calculate the HF distribution and then scale it by the relative HF(v=4) concentration to get an overall relative contribution to HF(v) for reaction 1a. After subtracting this distribution from the observed distribution, the NF(X) to NF($a^1\Delta$) ratio is 1:12. Combining this with the $b^1\Sigma^+$:$a^1\Delta$ ratio gives an estimate of the overall branching ratio of $X^3\Sigma^-$:$a^1\Delta$:$b^1\Sigma^+$ of 0.07:0.91:0.02. The estimate of NF(X) is *very* uncertain and may be in error by a factor of 2–3; the 0.07 value probably is an overestimate.

Energy Disposal for the HF + NF($a^1\Delta$) Channel. The vibrational energy disposal for this reaction is typical of unimolecular decomposition reactions[26] and is especially similar to other HX elimination reactions. Several authors have found that three- and four-centered HX eliminations release a moderate to high fraction of the available energy to translation and smaller amounts as internal excitation.[26–29] The mean fraction of vibrational energy for NF and HF are $\langle f_V(\mathrm{HF}) \rangle \approx 0.12$ and $\langle f_V(\mathrm{NF}) \rangle \lesssim 0.05$ which are consistent with these general findings. The $\langle f_V \rangle$ value for HF strongly depends on the estimate for $v = 0$; however, both methods used in Table I gave similar results. In previous studies[5,30] we have shown that, if HF(v) is formed in levels above $J = 10$, these high J levels can be observed in the flowing-afterglow apparatus used in this work. Since emission from high J levels could not be observed from the H + NF_2 reaction, the rotational excitation of HF(v) must be minimal. If the rotational energy imparted to HF is small, conservation of angular momentum suggests that the NF(a) also will have low rotational energy. The HF(v) surprisal for a three-body prior was strongly nonlinear and was of no aid in interpretation of the data. the surprisal using the prior based on the total degrees of freedom (of HF and NF) is still nonlinear (see Figure 2); but, a smooth extrapolation to $f_V = 0$ was possible. this extrapolation supported the HF(v=0) population from extrapolating the ln P_V vs. E_V plot to $E_V = 0$.

Vibrational population inversions are very rarely observed for HX elimination reactions and $\langle f_V(\mathrm{HX}) \rangle$ normally is in the range of 0.15.[27,26] The value found here for H + NF_2 may be slightly lower than HF elimination from the halogenated methanes,[28] ethanes,[27] or HSF_5.[8] Without reliable data for the HF(v=0) population, further discussion about the vibrational energy disposal is speculation. However, the nonlinear surprisals in Figure 2 arise because the P_V values are too large for the higher v levels. This could be a consequence of the HF and DF formed by reaction 1a or some other experimental problem (note that these relative populations are quite low and small changes could have large effects). If the true P_V for high f_V should be lowered, the vibrational energy disposal to HF would be even smaller for the 1b channel. If the energy release were statistical, $\langle f_V(\mathrm{HF}) \rangle$ and $\langle f_V(\mathrm{NF}) \rangle$ would be ~0.09. Although $\langle f_V(\mathrm{HF}) \rangle$ is near the statistical value, the shape of P_V(HF) is not consistent with statistical partitioning and the NF product has much less that the statistical amount of energy. Since the sum of the HF and NF(a) mean fractions of vibrational and rotational energies are ≤0.25, a large fraction of the available energy must be released as translational energy. Such a specific energy release implies a high energy barrier for the reverse addition of NF($a^1\Delta$) to HF. Such a barrier is schematically shown in Figure 8.

Zamir and Levine[30] have provided a systematic information theoretic analysis of the HX vibrational distributions from HX elimination reactions. They find that nearly all examples could be fitted by a linear surprisal with a negative λ_V, which shows that the HX product received more than the statistical amount of energy. The analysis suggested that one constraint, on the vibrational energy released to HX, is enough to describe the energy disposal. They also introduced a sum rule to account for the partitioning of the excess energy and the potential energy, i.e., $\langle E_V \rangle = a(E - E_0) + bE_0$ where E_0 is the barrier energy for the reverse process, E is the total available energy, and a and b are constants. The H + NF_2 reaction appears to provide a counter example, because the HF(v) surprisal is not highly linear, the energy release to NF is very low and the translational energy is high. Possibly this is because E_0 is a sizeable fraction of $\langle E \rangle$ and the energy constraint in this case should be on E_T, i.e., a momentum constraint associated with repulsive release of the potential energy.

Conclusions

The chemiluminescence from the HF(v) and NF($a^1\Delta$) products from the H + NF_2 reaction have been used to study the rate constant at 300 K, the vibrational energy diposal to each product, and some spectroscopic properties (τ, ω_e, and $\omega_e\chi_e$) of NF($a^1\Delta$). The rate constant for H + NF_2 is only 1.3×10^{-11} cm^3 molecule^{-1} s^{-1} and care must be exercised if this reaction is to be used as a source of NF($a^1\Delta$) for subsequent kinetic study in a flow system. The work[31] reporting the anomalously large rate constant for excitation transfer from NF($a^1\Delta$) to Bi may have experienced some problems in this regard. the H + NF_2 reaction proceeds via an intermediate complex and the energy disposal is interpreted in terms of a unimolecular reaction. The reaction is unusual in that a electronically excited product is formed with a high branching fraction (>0.9) and because the vibrational energy in each product[32] can be observed. The energy disposal is rather specific, a high fraction goes to E_T, and this elimination reaction does not fit the model advocated by Zamir and Levine[30] that was based upon the HX(v) distributions from HX elimination of large organic molecules. We suspect that, as greater microscopic detail for unimolecular elimination reactions becomes experimentally available, more complex exit channel coupling effects[33] will be found and more complex models will be ultimately needed to describe the dynamics.

Acknowledgment. this work was supported by the National Science Foundation under Grant 77-21380. We thank the Aerospace Corporation for the gift of N_2F_4. We also thank Professor R. D. Levine for sending preprints of ref 30 and for an exchange of viewpoints on HX elimination reactions, and Dr. M. A. A. Clyne for sending preprints of ref 4b and 4c.

(28) J. C. Stephenson and D. S. King, *J. Chem. Phys.*, **69**, 1485 (1978).
(29) B. E. Holmes and D. W. Setser, *J. Phys. Chem.*, **79**, 1320 (1975).
(30) (a) E. Zamir and R. D. Levine, *J. Chem. Phys.*, **73**, 2680 (1980); (b) E. Zamir and R. D. Levine, *Chem. Phys.*, in press.
(31) G. A. Chapelle, D. G. Sutton, and J. I. Steinfeld, *J. Chem. Phys.*, **69**, 5140 (1978).
(32) J. C. Stevenson, S. E. Bialkowski, and D. S. King, *J. Chem. Phys.*, **72**, 1161 (1980). The multiphoton dissociation of CF_2CFCl followed by spectroscopic analysis of both CF_2 an CFCl is another example.
(33) R. J. Wolf and W. L. Hase, *J. Chem. Phys.*, **73**, 3010 (1980), and related work mentioned in references in this paper.